

Active cavity absolute radiometer based on high- T_c superconductors

*J. P. Rice, S. R. Lorentz, R. U. Datla,
L. R. Vale, D. A. Rudman, M. Lam Chok Sing
and D. Robbes*

Abstract. To implement the detector-based radiometric scale in the new Medium Background Infrared (MBIR) facility at the National Institute of Standards and Technology (NIST), we have developed an electrical-substitution cavity radiometer that can be operated just above liquid-nitrogen temperature. This MBIR active cavity radiometer (ACR) utilizes a temperature-controlled receiver cone and an independently temperature-controlled heat sink. Being a thermal-type detector, low noise and drift of the radiometer signal depends mainly on low-noise temperature control of the receiver and heat sink. Using high critical-temperature (T_c) superconducting thin-film temperature sensors in the active control loops, we have achieved closed-loop temperature controllability of better than 10 μ K at 89 K for a receiver having an open-loop thermal time constant of about 75 s. For a flux level of 1 μ W to 10 μ W, the rms noise floor over a measurement cycle time is below 20 nW. This is the lowest noise level yet reported for a liquid-nitrogen-cooled electrical-substitution radiometer, and it is the first demonstration of the use of high- T_c superconductors in such a radiometer. Potential uses for this ACR in the MBIR facility include absolute measurement of the broadband radiance of large-area 300 K cryogenic black-body sources, and absolute measurement of the spectral radiance of laser-illuminated integrating spheres for improved spectral responsivity measurements of infrared transfer standard radiometers.

1. Introduction

Electrical-substitution radiometers have been developed for a variety of radiometric measurement purposes, including, for example, measurement of the Stefan-Boltzmann constant, long-term monitoring of solar irradiance, and use as primary standards of optical power at national standards laboratories [1, 2]. They generally work by comparing the heating effect of optical power with electrical power in alternate cycles, thus allowing a measurement of optical power in terms of electrical measurements. A common design that utilizes an absorptive receiving cavity under active temperature control is the active cavity radiometer (ACR).

Our application is for an ACR to serve as the absolute detector for routine radiance measurements in the MBIR facility [3]. In this facility, the background temperature can be as low as 80 K, as it has a light-

tight, liquid-nitrogen-cooled shroud in a 1.3×10^{-5} Pa (1×10^{-7} Torr) vacuum chamber. One source to be routinely measured is a large-area black body (LABB) having an exit aperture of 10 cm diameter and a radiance temperature in the range 200 K to 350 K [3]. Another potential source would be the Lambertian output from a laser-illuminated integrating sphere [4], which could be used instead of a black-body source to calibrate the absolute spectral radiance responsivity of filter radiometers such as the thermal-infrared transfer radiometer (TXR) [5]. Such a source, illuminated using tunable lasers from outside the MBIR chamber, would provide a monochromatic, spectrally tunable, large-area Lambertian source of radiance. It could be viewed alternately by the ACR and the TXR in the MBIR facility, thereby calibrating the TXR against the NIST detector-based radiance scale as maintained by the ACR.

The ACR described here is designed to operate over a temperature range of 85 K to 90 K. Since the typical measurement in the 80 K background MBIR chamber will involve a source having a radiance temperature of 300 K or lower, a cooled detector is required for net flux transfer from the source to the detector. Thus, a room-temperature ACR cannot be used. Helium-cooled ACRs, typically operating below 10 K, have higher sensitivity than the ACR described here, but are unsuitable for our intended application because they

J. P. Rice, S. R. Lorentz and R. U. Datla: Optical Technology Division, National Institute of Standards and Technology, Gaithersburg, MD 20899, USA.

L. R. Vale and D. A. Rudman: Electromagnetic Technology Division, National Institute of Standards and Technology, Boulder, CO 80303, USA.

M. Lam Chok Sing and D. Robbes: GREYC-CNRS UPRESA 6072, Institut des Sciences de la Matière et du Rayonnement, Université de Caen, 14050 Caen Cedex, France.

would be susceptible to unwanted special systematic effects of their own. For example, if no window is used, a radiometer operating at a temperature near 10 K or below cryopumps the residual gas onto the receiver cavity walls. This would affect the cavity absorptance and would need to be characterized. If a window is used, the transmittance of the window for broadband, diffuse light would have to be characterized. A great deal of work would be required to make convincing corrections for either of these systematic effects to achieve our required absolute radiance uncertainty. The purpose of this paper is to show that sensitivity at the required level can be achieved in an ACR that operates at a high enough temperature that cryopumping is not an issue. The key improvement over previous designs [6] is the use of high-critical-temperature (T_c) superconductor sensors [7, 8].

2. Design

The MBIR ACR design is shown in Figure 1. The ACR with its fore-optics is designed to fit into a 15 cm diameter liquid-nitrogen cryostat. The fore-optics consist of a temperature-controlled baffle tube housing both the aperture stop and the field stop. These are precision apertures, the area of which can be measured at the NIST with low uncertainty [9]. Any diffraction corrections due to these apertures can also be calculated with low uncertainty [10]. Using the aperture diameters d_a and d_c , and spacing s , the radiometer has a nominal full field-of-view of $\theta_0 = 8^\circ$ (Figure 1 and example 1 of Table 1). When viewing an extended-source black

body such as the MBIR LABB in radiance mode (both field stop and aperture stop overfilled), the ACR cavity will receive a radiant flux level of about $10 \mu\text{W}$ from the source at temperature T of 300 K. As shown below, this ACR is capable of measuring this flux level with a contribution to the standard random uncertainty below 20 nW, or 0.2 %. Because radiance is proportional to T^4 , this corresponds to a standard uncertainty in the radiance temperature of one-quarter of the above value, i.e. 0.05 %. For a source temperature of 200 K, this flux level, and hence the ACR contribution to the random uncertainty, can be maintained at 0.05 % if s is reduced, increasing the full field-of-view to 18° . Table 1 summarizes these two examples, comparing the various geometrical parameters and the flux levels expected.

The heart of the ACR consists of an electroformed copper conical receiver cavity (Figure 1). It has an entrance diameter of 1 cm, an apex angle of 30° , a wall thickness of $50 \mu\text{m}$, and is coated on the inside with Aeroglaze Z302 specular-black paint (Lord Corporation) for high absorptance at visible and infrared wavelengths. The outside surface of the cavity is gold-coated and is surrounded by a gold-plated copper heat sink. The receiver is thermally and mechanically anchored to the heat sink at the outside front of the cavity through a 1 cm diameter, 1 mm long sleeve made from 0.127 mm thick Kapton HN film (Dupont). The heat sink is, in turn, thermally and mechanically anchored by stainless-steel screws to a copper plate maintained at a temperature near 77 K by contact with the liquid-nitrogen reservoir.

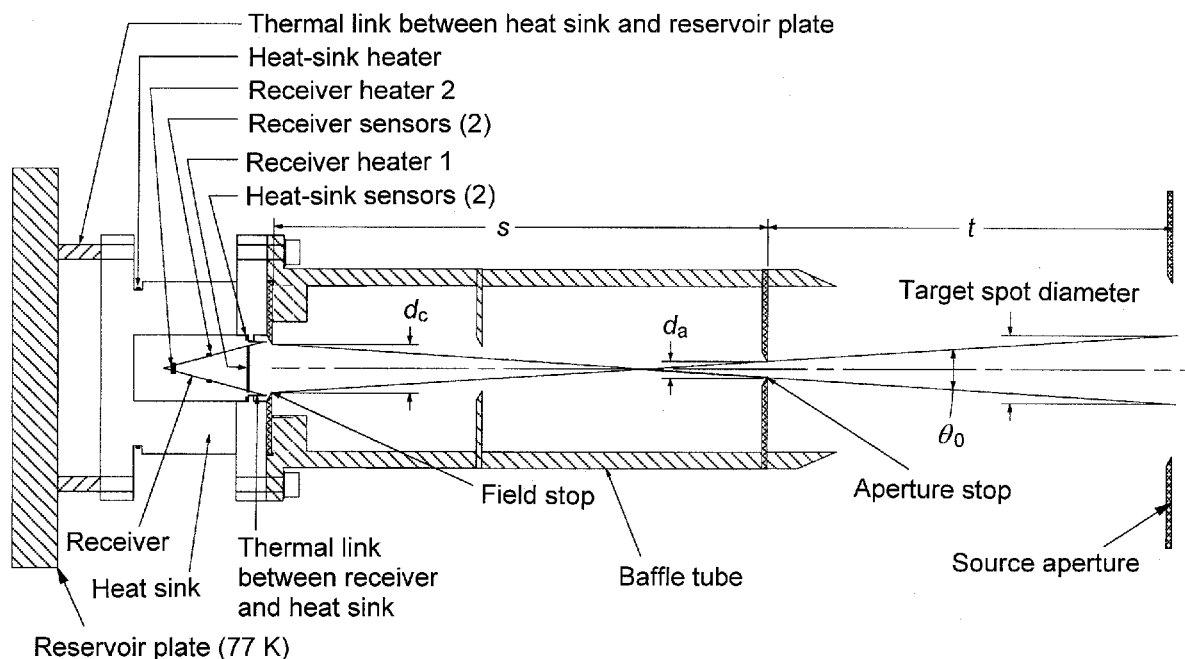


Figure 1. Design of the MBIR prototype ACR. For the tests reported here, a gold mirror was mounted in front of the receiver in place of the baffle tube and field stop, and optical power was simulated using electrical power applied to receiver heater 2 while the receiver was under active servo control through receiver heater 1.

Table 1. Two examples of possible fore-optics dimensions and the predicted approximate radiant flux levels entering the ACR receiver cavity.

| Dimension | Symbol | Example 1 | Example 2 |
|--|------------|-------------|-------------|
| Field-of-view | θ_0 | 8° | 18° |
| Aperture-stop diameter | d_a | 0.3 cm | 0.3 cm |
| Field-stop diameter | d_c | 1 cm | 1 cm |
| Spacing between aperture stop and field stop | s | 9.4 cm | 4.1 cm |
| Distance from aperture stop to source aperture for 4 cm target spot diameter | t | 27 cm | 12 cm |
| Flux from a 200 K black-body source | ϕ | 1.9 μ W | 10 μ W |
| Flux from a 300 K black-body source | ϕ | 10 μ W | 48 μ W |
| Flux from a 400 K black-body source | ϕ | 31 μ W | 150 μ W |

The heat sink and the receiver are both actively temperature-controlled by independent servo loops. To measure radiant power, the receiver is biased at a slightly higher operating temperature than the heat sink by applying a carefully measured electrical power to one of the heaters on the receiver. This electrical power is determined from the product of the measured voltage drop across the heater and the measured current through the heater. Then, when radiant power is applied, for instance, by opening a shutter in front of the ACR, the electrical power required to keep the receiver at a fixed temperature will drop, stabilizing to a new value. The difference in these electrical power measurements constitutes a measure of the radiant power. The measurement is absolute, provided that errors from sources such as shutter emittance, incomplete receiver absorptance, and nonequivalence between electrical and radiant power are small and quantifiable so that they can be corrected. Note that the calibration does not depend on a calibration of the sensors against a temperature scale, and that sensitivity over only a narrow temperature range is required.

The key to achieving low-noise measurements in an active cavity radiometer is to obtain low-noise temperature control of both the receiver and the heat sink. Based on our earlier studies [7, 8], we used thin-film sensors made from the high- T_c superconductor $YBa_2Cu_3O_{7-\delta}$ (YBCO), for which $T_c = 89$ K. The sensors each consist of a patterned bilayer of gold (for contacts) over YBCO on a $LaAlO_3$ (LAO) substrate. They were made in a standard process that involves laser-ablation of YBCO, *in situ* sputtering of gold, and photolithography coupled with ion-milling for pattern definition [11]. A single die was made and diced into several 1 mm \times 1 mm \times 0.5 mm chips. Each chip consists of a single, four-wire YBCO strip with four gold contact pads. Chips having two different resistor pattern designs were used, to provide sensors having two different resistance values at the transition midpoint. This was done to allow future tests to

be made of the dependence of the sensor noise on resistance. Both designs consist of a single line of YBCO having a nominal film thickness of 80 nm and length (between the voltage taps) of 600 μ m. However, sensors of Design 1 have a line width of 40 μ m and sensors of Design 2 have a line width of 10 μ m. Two sensors, one of each design, are bonded to the receiver cone (Figure 1). Similarly, two sensors, one of each design, are bonded to the heat sink near the receiver thermal link. For the characterizations reported below, only the sensors of Design 2 (receiver sensor 2 and heat-sink sensor 2) were used. Also, two wire-wound heater coils are bonded to the receiver cone, and one wire-wound heater and a calibrated platinum resistance thermometer (PRT) are bonded to the heat sink. Stycast 2850FT epoxy is used for bonding. All heaters and temperature sensors are four-wire devices. The sixteen leads leading to the receiver are connected to the heat sink. These leads are gold wires having a diameter of 13 μ m, except for the four heater current leads which are 25 μ m in diameter. The leads make electrical contact to the sensors and receiver heaters through pressed indium. The joule heating in the leads will present a systematic error in the measurement. However, this can be reduced to negligible levels by using a receiver heater resistance much higher than the lead resistance. In the present prototype the receiver heater resistances were near 50 Ω . Future versions will have receiver resistances ten to a hundred times greater. Alternatively, superconducting leads made of, for instance, the superconductor $Bi_2Sr_2Ca_2Cu_3O_{10}$ ($T_c \approx 110$ K) are conceivable, but are only now becoming commercially available.

3. Characterization

For tests of the intrinsic performance, a gold mirror was mounted on the front of the ACR in place of the field stop and baffle tube shown in Figure 1 so that the receiver viewed a reflection of itself. This gold mirror was made on a polished nickel-buffered aluminium substrate and was in good thermal contact with the heat sink, so that it was temperature-stabilized near 90 K. The tests reported here were made in a cryostat with the ACR in a stainless-steel vacuum-can that was, in turn, surrounded by liquid nitrogen. This provided a 1.3×10^{-4} Pa (1×10^{-6} Torr), 77 K background environment.

For the tests reported here, the resistances of the YBCO sensors were monitored by one of two ac resistance bridges (Linear Research LR-700). These provide constant-current-amplitude sine-wave excitation at 16 Hz (for the receiver sensor) or 19 Hz (for the heat-sink sensor). The resistance versus temperature of the YBCO sensors of Design 2 is shown in Figure 2. For these measurements, the heat-sink temperature, as read by the PRT using an LR-400 ac resistance bridge, was slowly varied so that the receiver temperature stayed close to the heat-sink temperature.

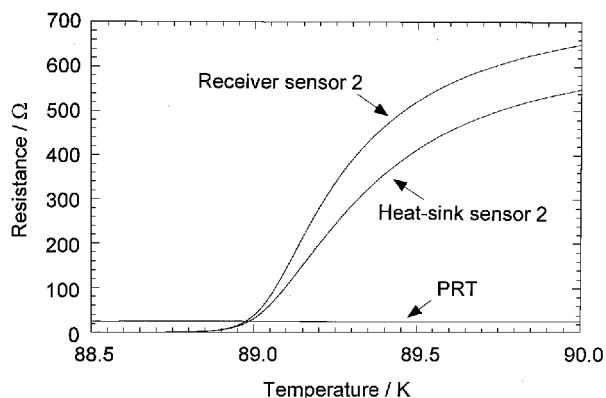


Figure 2. Resistance versus temperature at the superconducting transition of the YBCO sensors. These data were taken with an ac sine-wave excitation current of 10 μA amplitude. At 89.07 K, the change of resistance with temperature is 810 Ω/K and 1300 Ω/K for the heat sink and receiver sensors, respectively. For comparison, the resistance versus temperature of the PRT (0.43 Ω/K) is shown.

Table 2. Measured values for various parameters of the MBIR prototype ACR at 89 K.

| Parameter | Value | Uncertainty (1 σ) |
|---|------------------|------------------------------|
| Thermal time constant for receiver warming | 71 s | |
| Thermal time constant for receiver cooling | 74 s | |
| Thermal conductance between receiver and heat sink | 0.998 mW/K | |
| Heat capacity of receiver | 72.5 mJ/K | |
| Mass of painted receiver cavity | 245 mg | |
| Electrical resistance of receiver heater 1 | 53.7996 Ω | 0.0005 Ω |
| Electrical resistance of receiver heater 2 | 52.3735 Ω | 0.0005 Ω |
| Thermal time constant for heat-sink warming | 58.35 min | |
| Thermal time constant for heat-sink cooling | 65.55 min | |
| Thermal conductance between heat sink and reservoir | 29.5 mW/K | |
| Heat capacity of heat sink | 110 J/K | |
| Mass of heat sink | 297 g | |
| Electrical resistance of heat-sink heater | 70 Ω | |

These data showed the superconducting transition at a critical temperature (T_c) of 89 K with a 10 % to 90 % transition width of 0.6 K. This is typical for high-quality YBCO films. The transition width showed dependence on the current amplitude, since at higher currents the critical current is reached at a lower temperature.

Measurements of various thermal and electrical parameters are listed in Table 2. For measurements of the open loop thermal time constants τ , a step increase or decrease was made to the heater power for either the heat sink or receiver, and for each case the resulting temperature change versus time was fitted to an exponential form, yielding the parameters listed. The

thermal conductance G of the thermal links between receiver and heat sink, and between heat sink and reservoir, were determined from the change in applied power required to make a measured change in the receiver (or heat-sink) temperature. The heat capacity C was calculated as $C = G\tau$ using the average value for τ .

Data from a test of the ACR with the sensors in resistive-edge mode are shown in Figure 3. Using a commercial temperature controller (Linear Research LR-130) providing power to its heater, the heat sink was stabilized at a heat-sink sensor 2 resistance of 75 Ω . Using a separate LR-130 temperature controller providing power to receiver heater 1, the receiver was stabilized at a receiver sensor 2 resistance of 125 Ω , corresponding to a temperature slightly higher than the heat sink. The voltage across receiver heater 1 was monitored by an accurate voltmeter and, using the known resistance of this heater, the electrical power was determined and plotted versus time in Figure 3. At about 40 min into the test, about 10 μW of electrical power was applied by a stable voltage source to receiver heater 2 to simulate the thermal effect of opening a shutter. The receiver temperature controller reacted by decreasing the electrical power supplied to heater 1 in order to maintain a constant receiver temperature. At about 70 min the power to heater 2 was shut off, simulating the closing of a shutter, and the receiver temperature controller increased the electrical power to heater 1 to its original value. The difference in electrical power supplied to heater 1 during the shutter-closed and shutter-open phases is a measure of simulated radiant power, in this case supplied by heater 2. Figure 3 shows the raw data: no drift subtraction was necessary. Subtracting the shutter-open data from the shutter-closed data and propagating the standard deviation of the time series of stable measurements from all three phases of the cycle gives a measured heater 1 electrical power change of 9.03 $\mu\text{W} \pm 0.02 \mu\text{W}$. The simulated radiant power applied, as determined from the measured resistance of heater 2 and the voltage measured across the voltage taps of heater 2 during the shutter-open phase, was 9.0013 μW . The small difference is just outside the 1 σ measurement uncertainty. However, the entire difference can be explained by accounting for the joule heating of the gold current leads of heater 2. As explained above, the use of much higher heater resistances in future versions of this ACR will considerably reduce the effect of joule heating. Thus, the electrical-optical nonequivalence, as best as can be determined without actual optical measurements, will be negligible compared with the 0.2 % standard uncertainty that is a result of the noise.

4. Operating modes

In the tests described here, ACR servo control was based on monitoring temperature through the superconductive resistance edge of the sensors,

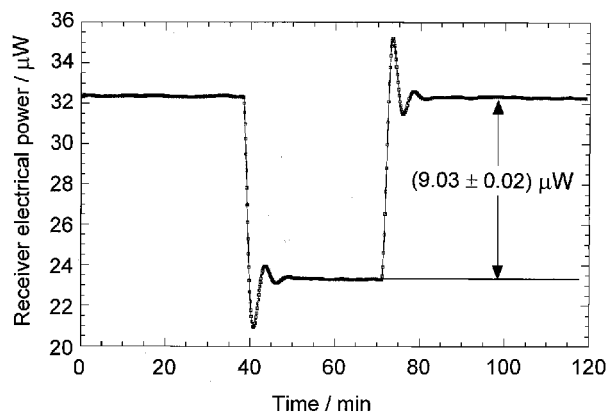


Figure 3. An example of uncorrected data for a measurement of about $10 \mu\text{W}$ of power with a random uncertainty of about 0.2 %. In this case, the measurement time was made exceptionally long to demonstrate the lack of significant drift. The settling following changes in electrical power results from the use of an analogue temperature-control loop. This can be reduced with the implementation of a shutter-synchronized digital temperature-control loop.

where the material passes from the normal state to the superconducting state near T_c . At least two other approaches using superconductive sensors are conceivable, which differ in the temperature-dependent quantity monitored.

One approach involves monitoring the kinetic inductance of a superconductor just below T_c [12]. The other involves monitoring the critical current of the sensor [8]. The critical current is the value of current that drives a superconductor into the normal state at temperatures below T_c . It is a strong function of temperature in YBCO a few degrees below T_c . It can be implemented using the same sensors as used here, but with specially designed room-temperature electronics to provide low-noise measurement of the critical current. This operating mode can be used to increase the maximum measurable radiant flux of the ACR since the greatest variation of critical current with temperature occurs several degrees below T_c . For example, Figure 2 shows that the maximum temperature difference between heat sink and receiver is about 1 K before one of the sensors can no longer be biased at its resistive edge. From the G listed in Table 2, this corresponds to a maximum of 1 mW of optical power. However, using critical current edge mode, the heat sink could be stabilized several degrees below T_c , enabling several milliwatts to be measured without making any changes to the cryogenic hardware.

5. Conclusion

A prototype ACR operable at liquid-nitrogen temperature has been designed and built for use in the NIST

MBIR facility. It is capable of providing absolute measurements of radiant flux levels ranging from $10 \mu\text{W}$ to several milliwatts with a standard uncertainty below 0.2 %. This is the first demonstration of the use of high- T_c superconductors in such a radiometer.

Acknowledgement. We thank G. Beatty for assistance with the YBCO sensor fabrication.

Note. References are made to certain materials and products in this paper to adequately specify the experimental procedures involved. Such identification does not imply recommendation or endorsement by the National Institute of Standards and Technology, nor does it imply that these products are the best for the purpose specified.

References

- Hengstberger F., *Absolute Radiometry*, San Diego, Academic Press, 1989.
- Parr A. C., A National Measurement System for Radiometry, Photometry, and Pyrometry Based Upon Absolute Detectors, *NIST Tech. Note 1421*, 1996.
- Fowler J. B., Johnson B. Carol, Rice J. P., Lorentz S. R., The new cryogenic vacuum chamber and black-body source for infrared calibrations at the NIST's FARCAL facility, *Metrologia*, 1998, **35**, 323-327.
- Lykke K. R., Shaw P.-S., Hanssen L. M., Eppeldauer G. P., Development of a monochromatic uniform source facility for calibration of radiance and irradiance detectors from $0.2 \mu\text{m}$ to $12 \mu\text{m}$, *Metrologia*, 1998, **35**, 479-484.
- Rice J. P., Johnson B. C., The NIST EOS thermal-infrared transfer radiometer, *Metrologia*, 1998, **35**, 505-509.
- Morozova S. P., Lisiansky B. E., Morozov P. A., Sapritsky V. I., Melenevski U. A., Petic A. G., New Low-Cost Absolute Cryogenic Radiometer for Space Black-Body Models Calibration, preprint.
- Rice J. P., Zhang Z. M., Liquid-Nitrogen-Cooled High T_c Electrical Substitution Radiometer as a Broadband IR Transfer Standard, *NIST Tech. Note 1414*, 1996.
- Lam Chok Sing M., Rice J. P., Dolabdjian C., Robbes D., Low-Noise Temperature Control Using a High T_c Superconducting Sensor Compared to a Conventional PRT Method, *Proc. European Conference on Applied Superconductivity*, 1997, in press.
- Fowler J. B., Durvasula R. S., Parr A. C., High-accuracy aperture-area measurement facilities at the National Institute of Standards and Technology, *Metrologia*, 1998, **35**, 497-500.
- Shirley E. L., Datla R. U., *J. Res. Natl. Inst. Stand. Technol.*, 1996, **101**, 745-753.
- Stork F. J. B., Beall J. A., Roshko A., DeGroot D. C., Rudman D. A., Ono R. H., Krupka J., Surface resistance and morphology of YBCO films as a function of thickness, *IEEE Trans. Appl. Supercond.*, 1997, **7**, 1921.
- McDonald D. G., Novel Superconducting Thermometer for Bolometric Applications, *Appl. Phys. Lett.*, 1987, **50**, 775-777.